The Cryosphere, 17, 391–405, 2023
https://doi.org/10.5194/tc-17-391-2023

The Cryosphere Open Access EGU

200-year ice core bromine reconstruction at Dome C (Antarctica): observational and modelling results

François Burgay[1,2], Rafael Pedro Fernández[3], Delia Segato[2,4], Clara Turetta[2,4], Christopher S. Blaszczak-Boxe[5], Rachael H. Rhodes[6], Claudio Scarchilli[7], Virginia Ciardini[7], Carlo Barbante[2,4], Alfonso Saiz-Lopez[8], and Andrea Spolaor[2,4]

[1]Paul Scherrer Institute, Laboratory of Environmental Chemistry (LUC), 5232 Villigen PSI, Switzerland
[2]University Ca' Foscari of Venice, Department of Environmental Sciences, Informatics and Statistics, 30172 Venice Mestre, Italy
[3]Institute for Interdisciplinary Science, National Research Council (ICB-CONICET), FCEN-UNCuyo, Mendoza 5501, Argentina
[4]National Research Council, Institute of Polar Sciences, 30172 Venice Mestre, Italy
[5]Interdisciplinary Studies Department, Howard University, 20059 Washington, DC, United States
[6]Department of Earth Sciences, University of Cambridge, Cambridge, United Kingdom
[7]Laboratory of Observations And Measures for the Environment and Climate (SSPT-PROTER-OEM), ENEA, Rome, Italy
[8]Department of Atmospheric Chemistry and Climate, Institute of Physical Chemistry Rocasolano, CSIC, Madrid, Spain

Correspondence: Andrea Spolaor (andrea.spolaor@unive.it)

Received: 1 July 2022 – Discussion started: 2 September 2022
Revised: 11 January 2023 – Accepted: 12 January 2023 – Published: 27 January 2023

Abstract. Bromine enrichment (Br_{enr}) has been proposed as an ice core proxy for past sea-ice reconstruction. Understanding the processes that influence bromine preservation in the ice is crucial to achieve a reliable interpretation of ice core signals and to potentially relate them to past sea-ice variability. Here, we present a 210 years bromine record that sheds light on the main processes controlling bromine preservation in the snow and ice at Dome C, East Antarctic plateau. Using observations alongside a modelling approach, we demonstrate that the bromine signal is preserved at Dome C and it is not affected by the strong variations in ultraviolet radiation reaching the Antarctic plateau due to the stratospheric ozone hole. Based on this, we investigate whether the Dome C Br_{enr} record can be used as an effective tracer of past Antarctic sea ice. Due to the limited time window covered by satellite measurements and the low sea-ice variability observed during the last 30 years in East Antarctica, we cannot fully validate Br_{enr} as an effective proxy for past sea-ice reconstructions at Dome C.

1 Introduction

Halogens play an important role in the chemistry and oxidising capacity of the Earth's atmosphere: they take part in new particle formation processes, promote mercury oxidation, influence the budget of HO_x and NO_x radicals, and cause ozone depletion through efficient catalytic cycles (Saiz-Lopez and Von Glasow, 2012; Simpson et al., 2007). Volcanic eruptions (Gutmann et al., 2018) and the ocean (Parrella et al., 2012; Prados-Roman et al., 2015) represent the main natural sources of halogens to the atmosphere, releasing significant amounts of bromine (Br) and iodine (I) (Cuevas et al., 2018; Carpenter et al., 2013). In this work, we focus on bromine, which has been shown to dominate halogen emissions and chemistry in the polar atmosphere through the so-called "bromine explosion events" (Pratt et al., 2013; Platt and Lehrer, 1997). These are heterogeneous autocatalytic photochemical reactions, which were first described in the Arctic boundary layer and that cause the bromine-induced ozone depletion events (Fan and Jacob, 1992; Vogt et al., 1996; Foster et al., 2001; Wennberg, 1999; Barrie et al., 1988; Kreher et al., 1997). These autocatalytic mul-

tiphase chain reactions require both acidic conditions and sunlight to produce an exponential increase in atmospheric bromine concentration, mainly as gaseous BrO, Br_2, and HOBr (Schönhardt et al., 2012; Zhao et al., 2016; Nghiem et al., 2012). In the polar regions, the most favourable substrate (i.e. with a large bromide content) to produce such bromine explosion and ozone depletion events during springtime is the sea salt aerosol derived from surface blowing snow deposited over first-year sea ice (FYSI), which is characterised by acidic conditions, higher Br^- / Cl^- ratio (Pratt et al., 2013), and higher salinity than the snow deposited over multi-year sea ice (MYSI) (Frey et al., 2020). Direct observations from two winter cruises in the Weddell Sea (Antarctica) and model simulation showed that significant bromine losses take place in the aerosol phase, indicating that sea salt aerosol debromination from salty blowing snow over sea ice represents a relevant source of gas-phase inorganic bromine to the troposphere (Frey et al., 2020; Parrella et al., 2012; Yang et al., 2005). Note that most inorganic bromine gasses present in the atmosphere are highly water-soluble and they suffer wet and dry deposition over the ice sheets (Legrand et al., 2021; Parrella et al., 2012; Fernandez et al., 2019).

Especially during the "bromine explosion events", bromine, that shares the same sources as sodium (i.e. sea salt), is significantly enriched compared to sodium (Na) in the FYSI surfaces, exceeding the bromine-to-sodium mass ratio of seawater (Millero et al., 2008). Being promoted by the presence of FYSI compared to MYSI, this bromine enrichment (Br_{enr}, Eq. 1) has been proposed as a potential tracer for the reconstruction of past FYSI conditions (Spolaor et al., 2013b, 2016; Maffezzoli et al., 2019; Vallelonga et al., 2017). Qualitatively, higher Br_{enr} values were linked to larger FYSI extent (Spolaor et al., 2013b). However, many unknowns, mainly related to the source, transport, and preservation of bromine within the snowpack, still remain (Maffezzoli et al., 2019). For example, it has been suggested that the anthropogenic-induced acidity increase of the snow deposited over the sea-ice surface can enhance the sea salt debromination rates enhancing the release of reactive bromine from sea salt aerosols into the atmosphere (Maselli et al., 2017; Sander et al., 2003). Further, bromine can also be re-emitted from the snowpack after deposition and prior to burial. However, the results obtained from previous studies are contradictory and site-specific (Mcconnell et al., 2017; Legrand et al., 2016; Dibb et al., 2010; Spolaor et al., 2019). In Greenland, Dibb et al. (2010) showed that bromine photoactivation was present during spring/summer and highlighted an efficient Br chemical cycling above the snow. In the Svalbard Archipelago, a high-temporal resolution study designed to investigate the potential photoemission of bromine from the snowpack (Spolaor et al., 2019) did not highlight any bromine diurnal cycle, suggesting its preservation in snow. In Antarctica, through the investigation of Na and Br fluxes against snow accumulation rate, McConnell et al. (2017) found that bromine re-emission from the Antarctic snowpack is inversely dependent on the accumulation rate. It was shown that the bromine loss from the snowpack was higher (65 %) at sites with the lowest accumulation rate ($50\,kg\,m^{-2}\,yr^{-1}$), and it decreased to 11 % at sites with high annual accumulation rate ($300\,kg\,m^{-2}\,yr^{-1}$). Based on these observations, virtually all bromine deposited at Dome C (Antarctica), where the annual snow accumulation is ≈ 25–$28\,kg\,m^{-2}\,yr^{-1}$, would have been re-emitted to the atmosphere prior to burial (Mcconnell et al., 2017; Maffezzoli et al., 2019). These conclusions contrast with previous observations performed at Dome C that reported no significant bromine re-emission from the snowpack (Legrand et al., 2016). An additional process that can affect bromine preservation within the snowpack has been identified in coincidence with the 17.7 ka Mt. Takahe volcanic eruption, when the combination of an increased surface ultraviolet (UV) radiation, due to stratospheric ozone depletion, and high acidity conditions was associated with a decrease in ice bromine concentration (Mcconnell et al., 2017). To our knowledge, there are no investigations that focused on the effects of the modern UV radiation changes reaching the Antarctic plateau, due to the ozone hole formation, on bromine preservation in snow.

To unravel the physicochemical processes that can influence bromine preservation in the snow, we investigated the main pathways that can induce its emission from the snowpack to the atmosphere. Bromine is mainly present in the Antarctic snowpack as bromide (Spolaor et al., 2013a) and it can be oxidised by OH radicals (George and Anastasio, 2007; Abbatt et al., 2010) to form evaporable gaseous bromine. The main $^{\bullet}OH$ source within the snowpack is the photolysis of hydrogen peroxide (Chu and Anastasio, 2005), nitrate (Chu and Anastasio, 2003; Abbatt et al., 2010), and nitrite (Chu and Anastasio, 2007). Understanding the relevance of each of these photochemical pathways in explaining the preservation of bromide in the Antarctic snowpack before and after the onset of the modern-ozone hole is then crucial for a reliable interpretation of the bromine enrichment profile observed in ice core records.

In this study, we present the first bromine record retrieved from a shallow firn core collected at Dome C, Antarctica, covering the period 1800–2012. Through the evaluation of the bromine profile, it is possible to provide new evidence about the role of the enhanced solar UV radiation due to the onset of the modern Antarctic ozone hole (1975) on bromine preservation in the snowpack. An extended evaluation of the role of $^{\bullet}OH$ precursors and their relevance at Dome C is also performed. Lastly, an assessment of the suitability of Br_{enr} as a potential past sea-ice tracer at Dome C is also addressed by combining air-mass transport reanalysis and sea-ice extent satellite observations. The results presented in this paper open new perspectives on future long-term bromine studies from ice cores retrieved from low accumulation areas, aimed at forecasting future deep core drillings at Dome C, such as those planned for the Beyond EPICA project.

2 Material and methods

2.1 Ice core sampling and location

A 13.72 m shallow ice core was drilled close to Concordia Station, at Dome C (3233 m a.s.l.; 75°05′59″ S, 123°19′56″ E) in 2012. The retrieved shallow ice core covers approximately 212 years, from 1800 to 2012. The ice core dating is described in detail by Spolaor et al. (2021), with age uncertainties ranging from 1 year at surface to 5 years at the bottom of the core. Dome C is a suitable Antarctic site for performing photochemical studies related to the preservation of reactive elements and halides within the snowpack (Savarino et al., 2007; Cairns et al., 2021; Song et al., 2018; Spolaor et al., 2018, 2021). This location presents a low and rather constant accumulation rate ($25.3 \pm 1.3\,\mathrm{kg\,m^{-2}\,yr^{-1}}$ from 1816–1998, $28.3 \pm 1.3\,\mathrm{kg\,m^{-2}\,yr^{-1}}$ from 1965–1998, $28\,\mathrm{kg\,m^{-2}\,yr^{-1}}$ from 2004–2011) (Frezzotti et al., 2005, 2013; Genthon et al., 2016), and it is located about 1000 km away from shorelines, thus not being directly affected by local coastal emissions. Matching these criteria is essential for the evaluation of the effects of modern stratospheric ozone loss due to long-lived ozone depleting substances in the potential bromine release from the snowpack.

The shallow ice core was collected using a hand drill (3 in. diameter); the sections were sealed in plastic containers and shipped to the Institute of Polar Sciences of the National Research Council (ISP-CNR) in Venice (Italy). The ice core sections were subsequently sampled at 5(±1) cm resolution (corresponding to approx. 1 year) using a ceramic knife, rinsed with Ultra Pure Water (UPW, Elga Lab, UK) after each use. Only the central part of the core was collected into 50 mL pre-cleaned polyethylene (PE) vials for subsequent analyses, while the outer 2 cm was removed by scraping with a ceramic knife. The core samples were processed in a class 1000 inorganic clean room under a class 100 laminar-flow bench. Samples were kept at −20° C and under dark conditions until the analysis to avoid any possible photolysis reaction. Since we were only interested in the water-soluble bromine and sodium fractions and to avoid potential halogen loss (Flores et al., 2020), the analyses were conducted on melted and not acidified samples by inductively coupled plasma sector field mass spectrometry (ICP-SFMS; see Sect. 2.2). The sodium record considered in this study had some gaps from 1989–1997 ($n = 12$, corresponding to 5 % of the total amount of samples) that were filled with Na concentration data retrieved from two snow pits collected in 2013 and 2017, as reported in Spolaor et al. (2021).

2.2 Instrumental analysis and cleaning procedure

Total sodium and bromine concentrations were determined by ICP-SFMS following Spolaor et al. (2016). Each analytical run started and ended with an Ultra-Pure Water (UPW) cleaning session of 3 min to ensure a stable background level throughout the analysis. The external standards that were used to calibrate the analytes were prepared by diluting a 1000 ppm stock IC (ion chromatography) standard solution (TraceCERT® purity grade, Sigma-Aldrich, MO, USA). The standard concentrations ranged between 1 and $200\,\mathrm{ng\,g^{-1}}$ for sodium and 0.05 and $0.200\,\mathrm{ng\,g^{-1}}$ for bromine. As for the samples, the standards were not acidified. Precision and accuracy of the measurements were determined through the multiple reading of selected ice samples and external standards, respectively. The relative standard deviation (RSD %) was low for all the analytes, ranging between 3–4 % for sodium and 5–7 % for bromine, while accuracy, expressed as the ratio between the observed and the true values, was 105 % for sodium and 92 % for bromine. The instrumental limit of detection (LoD), calculated as 3 times the standard deviation of the blank ($n = 10$), was $1\,\mathrm{ng\,g^{-1}}$ for Na and $0.05\,\mathrm{ng\,g^{-1}}$ for Br. Bromine and sodium concentration values were used to calculate bromine enrichment ($\mathrm{Br_{enr}}$) as follows:

$$\mathrm{Br_{enr}} = \frac{[\mathrm{Br}]}{[\mathrm{Na}] \cdot 0.0062}, \quad (1)$$

where Br and Na are the concentrations obtained from the Dome C record, and 0.0062 reflects the bromine-to-sodium mass ratio in seawater (Spolaor et al., 2013b; Millero et al., 2008).

All the plastic material used for sample storage and analysis was washed 5 times using UPW and filled with UPW for 1 week. Then, it was rinsed again 5 times with UPW and dried under class-100 laminar flow hood before use.

2.3 Back-trajectories calculation, satellite observations, and statistical analysis

Backward air mass trajectories that reach the Dome C site (75°05′59″ S, 123°19′56″ E) were calculated to identify the most likely ocean and sea-ice areas that release bromine species to the atmosphere and that can be transported to the interior of Antarctica. Back-trajectories were obtained from the Hybrid Single-Particle Lagrangian Integrated Trajectory (HYSPLIT) model (Stein et al., 2015) using European Centre for Medium-range Weather Forecasts (ECMWF) ERA5 meteorological reanalysis (Hersbach et al., 2020). ERA5 is available on 37 pressure levels with a regular spatial grid of 0.25° × 0.25° at hourly temporal sampling. However, due to the huge amount of trajectories needed for this study, for computation requirements, we considered ERA5 parameters on a spatial grid of 0.5° × 0.5° every 3 h and 24 pressure levels (Becagli et al., 2022). Five-day backward trajectories were calculated every 3 h at 1000, 2000, and 3000 m above Dome C model terrain height for the period 1979–2018. Each back trajectory was then projected on the sea-ice concentration field (SIC) and the 10 m wind field (still in the ECMWF ERA5 reanalysis), associating each value along the trajectory path with the nearest SIC and wind speed val-

ues. The main paths of air masses reaching Dome C were highlighted dividing the Southern Hemisphere in a regular $1° \times 1°$ mesh and counting the total number of back-trajectories points at 5 d, falling in each grid cell (i.e. the hours spent by the air mass in each grid cell). Since bromine species are emitted in the marine boundary layer (MBL) (Sander et al., 2003), source bromine areas were evaluated, selecting only the trajectory where the air mass paths lie within the MBL and over sea ice and counting the total number of resulting points, where conditions are fulfilled, in each of the $1° \times 1°$ grid cells. The height of MBL was set equal to the 900 hPa isosurface (Lewis et al., 2004) and a value of SIC >15 % was considered in order to simulate the presence of the sea-ice cover (Becagli et al., 2022). The sea-ice concentrations used in this work are derived from passive-microwave radiometers on NASA's satellites. The data are publicly available at the NASA Earth Science portal (https://earth.gsfc.nasa.gov/, last access: 15 March 2022) and at the National Snow and Ice Data Center portal (http://nsidc.org, last access: 15 March 2022). The sea-ice extents (in km^2) are calculated as the hemispheric total as well as five regions in the Southern Ocean (Indian Ocean, Western Pacific, Ross Sea, Bellingshausen and Amundsen seas, and the Weddell Sea).

The correlations computed among the different variables of this study (Na, Br, Br_{enr}, sea-ice extent data, Southern Annular Mode (SAM) index) were performed using a 3 years moving average. This choice takes into account both the dating error of the core (≈ 3 years) and the effects of wind erosion on the age distribution of surface snow that spans over more than a year (Picard et al., 2019). To identify any abrupt change point in the records, the *findchangepts()* Matlab (Mathworks) function was used.

2.4 CAM-Chem model set-up

The wavelength-dependent solar ultraviolet (UV) radiation reaching the Antarctic plateau surface at Dome-C during the 1950–2010 period was computed using the Community Earth System Model (CESM) (Tilmes et al., 2016). The setup of the atmospheric component of the model (CAM-Chem, version 4) was identical to the one used in previous studies addressing the evolution of iodine ice core records in the Arctic (Cuevas et al., 2018) and Antarctica (Spolaor et al., 2021), and considers prescribed sea surface temperatures and sea-ice distributions following the CCMI-REFC1 recommendation (Eyring et al., 2013). The CAM-Chem VSL setup includes geographically distributed and seasonally-dependent natural oceanic emissions of five bromocarbons ($VSL^{Br} = CHBr_3$, CH_2Br_2, CH_2BrCl, $CHBrCl_2$, $CHBr_2Cl$) and four iodocarbons ($VSL^{I} = CH_3I$, CH_2ICl, CH_2IBr, CH_2I_2), whose oceanic flux is assumed to remain constant during the whole modelling period (Ordóñez et al., 2012). The chemical scheme includes the additional inorganic chlorine and bromine contribution arising from the so-called sea salt dehalogenation recycling occurring in the marine boundary layer and the free troposphere (Fernandez et al., 2014; Fernandez et al., 2021). The model was configured in free-running mode, with 26 vertical levels expanding from the Earth's surface to approximately 40 km (3.5 hPa in the upper stratosphere), and with a spatial resolution of 1.9° latitude by 2.5° longitude. The CAM-Chem REFC1 configuration used here provides a reasonable representation of the evolution of the size and depth of the ozone hole, presenting an excellent agreement with satellite ozone observations during the modelled period (Fernandez et al., 2017; Spolaor et al., 2021).

Here, we compute the photolysis rate constant (J-value) of different $^{\bullet}OH$ precursors involved in the preservation of bromine in the snowpack, following the same approach used in Spolaor et al. (2021). The molar absorptivities, quantum yields, and species concentrations for hydrogen peroxide, nitrate, and nitrite at Dome-C are summarised in Table 1. The modelled actinic flux reaching the Antarctic surface includes 100 bins expanding from 121 to 750 nm, with a spectral resolution ranging from less than 1 nm in the UV to 50 nm in the visible edge. In particular, the model bandwidth within the 280–400 nm spectral range considered in this work possesses a mean resolution of 4 nm. Thus, the CAM-Chem surface actinic flux for each wavelength grid was linearly interpolated into a 1 nm bandwidth, and the mean J-value during the whole sunlit period (i.e. from 1 September of a given year to 28 February of next year) was computed offline at the closest grid box to Dome C (74.84° S; 122.5° E; model mean altitude of 3300 m a.s.l.). The complete sunlit period (spring + summer) was selected because even when the largest changes in surface actinic flux associated with the ozone hole formation are observed during spring, the UV radiation intensity reaching the Antarctic plateau maximises during the summer (Spolaor et al., 2021).

3 Results and discussion

3.1 Sodium, bromine, and bromine enrichment profiles from the Dome C shallow core

Air masses arriving at Dome C originate from a vast area that extends over the eastern Antarctic Ocean, Ross Sea, and in minimal percentage from West Antarctica. Back trajectory analyses (Fig. 1) confirm that the most likely source areas of bromine and sodium emissions during the 1979–2018 period extend from the Indian Ocean sector (IO, 11 %) up to the Ross Sea sector (RS, 21 %), with the most likely area being the western Pacific sector (WP, 45 %), with the remaining 17 % from Bellingshausen and Amundsen seas (B and A) sector.

The variability in sodium concentration, a conservative tracer that does not show any post-depositional transformation, is used here to evaluate the marine contribution

Table 1. Summary of the $^{\bullet}$OH quantum yields for H_2O_2, NO_3^-, and NO_2^-, their molar absorptivities, and their concentration at Dome C.

Species	$^{\bullet}$OH quantum yield (Chu and Anastasio, 2007, 2005, 2003)	Concentration at Dome C
H_2O_2	0.7	$2\,ng\,g^{-1}$ (Frey et al., 2006)[b]
NO_3^-	0.0034 at pH = 5	$110\,ng\,g^{-1}$ (Spolaor et al., 2021)
NO_2^-	0.020 ($T = 260$ K, $\lambda = 280$ nm)	[a]$0.092\,ng\,g^{-1}$

[a] Estimated (more details in the text). [b] The value is reported from 3.5 m depth.

at Dome C (Caiazzo et al., 2021). Sodium concentrations along the entire record spanned from 12 to $117\,ng\,g^{-1}$, with an average value of $40 \pm 13\,ng\,g^{-1}$. Na profile (Fig. 2) shows an increase in concentration from 1800–1850, followed by a long-term decreasing trend until 1994. Over the last 18 years of the record, higher sodium concentrations were recorded, suggesting an enhanced transport towards Dome C. Bromine concentration at Dome C ranges from below the LoD ($0.05\,ng\,g^{-1}$) to $0.41\,ng\,g^{-1}$, with an average value of $0.10 \pm 0.05\,ng\,g^{-1}$ along the entire record. A significant bromine increase was detected since 2004 when Br concentration increased from $0.10 \pm 0.05\,ng\,g^{-1}$ (pre-2004) to $0.23 \pm 0.09\,ng\,g^{-1}$ (post-2004). The absence of an abrupt change of the bromine signal at the onset of the ozone hole (1975) indicates that Br is preserved in the snowpack independently on the incoming UV-radiation (see Sect. 3.2). Sodium and bromine did not show any significant correlation ($r = 0.06$, p-value $= 0.20$) along the entire record, suggesting different deposition velocities during transport from the coast, with sodium being deposited faster than bromine. Indeed, in the polar atmosphere, sodium is present in the aerosol phase and it is mainly affected by wet deposition processes. It was observed that its concentration decreases significantly with distance from the coast, reaching a rather constant deposition rate at approximately 400 km inland (Vallelonga et al., 2021). Contrarily, bromine exists in both the aerosol and in the gas phase, its atmospheric lifetime is also driven by dry deposition processes, it can experience heterogeneous chemical recycling during transport, and its concentration gradually decreases from 100–1000 km inland (Simpson et al., 2005; Vallelonga et al., 2021).

Br_{enr} values ranged between 0.07 and 1.6 with an average value of 0.4 ± 0.3 along the entire record. Contrarily to sodium and bromine, the enrichment did not show any significant increase in the recent part of the record. On the contrary, a significant regime change was detected in 1825, when the Br_{enr} mean value changed from 0.7 ± 0.3 (1800–1825) to 0.4 ± 0.3 (1825–2012). A two-sample t-test strengthened the significant difference between the two periods (p-value <0.001). In general, Br_{enr} values were mainly below 1 (i.e. bromine is depleted relative to sodium), which is expected at remote locations like Dome C, since the Br to Na ratio depends on the relative transport times of sea salt aerosol and gaseous bromine compounds in the atmosphere (Spolaor et al., 2013b; Simpson et al., 2007; Vallelonga et al., 2021). Thus, our findings agree with the synthesis of Vallelonga et al. (2021), which show low Br_{enr} values near the coast, a gradual increase at 300–600 km inland and a following decrease to values lower than 1 for all sites located more than 800 km from the coast. The few Br_{enr} values higher than 1 may indicate larger FYSI surface from the source areas (Spolaor et al., 2016) or different bromine partitioning between the aerosol and gas phase that depends on the aerosol size and, consequently, on atmospheric resident times (Legrand et al., 2016; Maffezzoli et al., 2019; Vallelonga et al., 2021). In addition, changes in background atmospheric $^{\bullet}$OH and NO_x might have had an impact on the gas-phase bromine partitioning between reservoir and reactive species that might have led to a faster bromine deposition, since species like $BrONO_2$ and HOBr have larger and more efficient deposition velocities than reactive species like BrO and Br (Saiz-Lopez and Fernandez, 2016; Fernandez et al., 2019).

In Antarctica, few other long-term bromine records exist and they were all collected from coastal sites (Spolaor et al., 2013b; Vallelonga et al., 2017). In contrast to Dome C, these records are more directly influenced by local marine contributions. The shorter atmospheric transport time from the source to the deposition location is reflected by the higher Br_{enr} values observed in these cores (Vallelonga et al., 2017).

3.2 Bromine preservation in the snowpack at Dome C

When reaching the snowpack, UV radiation can rapidly break weak chemical bonds and, due to its high energy, can promote photochemical reactions, especially in the UV-A (320–400 nm) and UV-B (290–320 nm) wavelength bands (Grannas et al., 2007). Due to its low accumulation rate, Dome C is the perfect location for performing UV photolysis studies on chemical species occurring at the ice and snow surface (Frey et al., 2009; Savarino et al., 2007). The stratospheric ozone layer depletion observed since 1975 has caused an increase in the incoming solar UV radiation over Antarctica at $\lambda < 300$ nm, enhancing, for example, the photochemical iodide oxidation and its subsequent release from the snowpack (Spolaor et al., 2021).

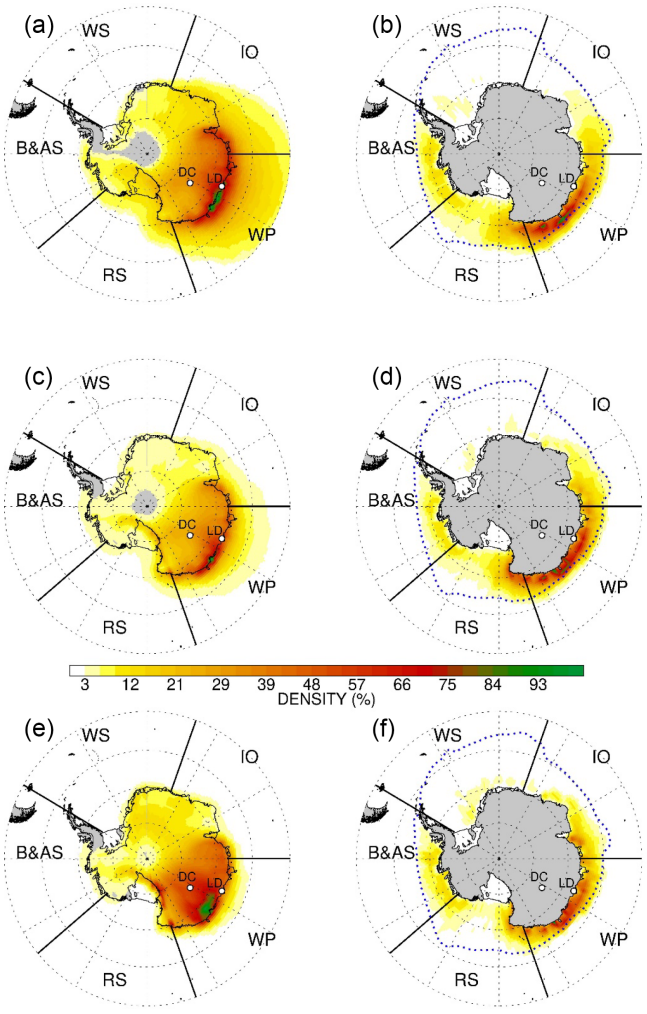

Figure 1. Five-day back-trajectory analysis of air masses arriving at the Dome C site for the period 1979–2018. The back trajectories are calculated at **(a, b)** 1000 m, **(c, d)** 2000 m, and **(e, f)** 3000 m above Dome C model terrain height for the period 1979–2018. Maps are divided into five sectors: Indian Ocean (IO, 20–90°), western Pacific Ocean (WP, 90–150°), Ross Sea (RS, 160–230°), and Bellingshausen and Amundsen seas (B and A, 230–20°). Panels **(a)**, **(c)**, and **(e)** represent the sum of the total number of backward-trajectory points (i.e. hours) within the fifth and the second days found in each 1° × 1° grid cell. Panels **(b)**, **(d)**, and **(f)** represent backward-trajectory points (i.e. hours) within the MBL that cross areas with >15 % sea ice concentration at the given point of time. Each contour is normalised from 0 to 100 rescaling with respect to its maximum values and resampled to 0.5° × 0.5° grid mesh in order to increase readability. The grey dashed line represents the median ice edge in September (maximum extent) over the period 1979–2018.

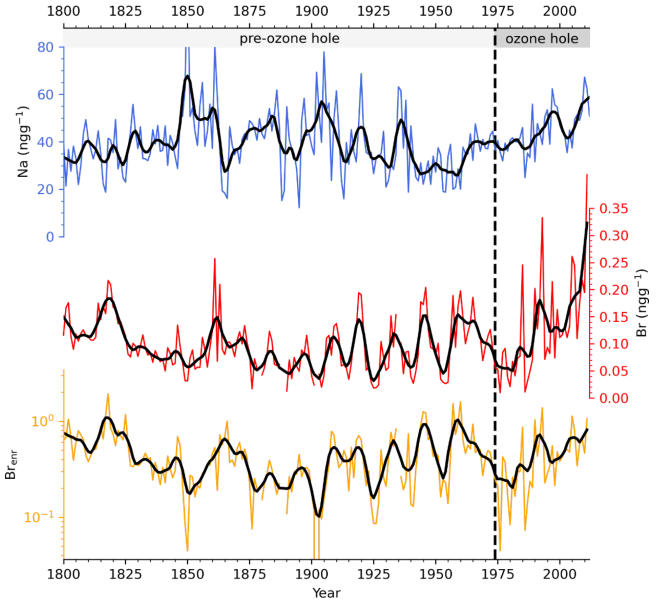

Figure 2. Sodium (blue line), bromine (red line), and bromine enrichment (yellow line) ice core record from 1800–2012. Thick lines refer to a smoothed 3-year moving average.

As highlighted in Sect. 3.1, no significant changes either in bromine concentration or in bromine enrichment have been detected at Dome C since 1975, suggesting that, contrarily to iodine (Spolaor et al., 2021), the ≈ 10-fold enhanced UV radiation reaching the Antarctic plateau has not altered bromine preservation within the snowpack (Fig. 2). Moreover, laboratory and chamber experiments showed enhanced photochemical oxidation and subsequent release of $I_{2(g)}$ from artificial snow/ice and the snowpack through the formation of a critical I-O_2 complex having an absorption band centred at 290 nm (Kim et al., 2016). At present, there is no evidence and/or available literature describing a similar Br-O_2 complex, and/or any other brominated intermediate product, that leads then to the release of $Br_{(2)(g)}$. In fact, the main inorganic route for bromide oxidation requires radical oxidants (e.g. $^{\bullet}$OH) to drive the redox production of hypobromous acid (BrOH) (Artiglia et al., 2017). This oxidised species can then combine with other reduced halide ions to form molecular halogen compounds that are released into the gas phase (Reactions R1–R4) (George and Anastasio, 2007) as follows:

$$Br^- + {}^{\bullet}OH \rightarrow {}^{\bullet}BrOH^- \quad (R1)$$

$${}^{\bullet}BrOH^- + Br^- \rightarrow {}^{\bullet}Br_2^- + OH^- \quad (R2)$$

$${}^{\bullet}Br_2^- + HO_2^{\bullet} \rightarrow Br_2 + HO_2^- \quad (R3)$$

$${}^{\bullet}Br_2^- + {}^{\bullet}Br_2^- \rightarrow Br_2 + 2Br^-. \quad (R4)$$

Over ice and snow substrates, hydroxyl radicals ($^{\bullet}$OH) can be produced by the photolysis of hydrogen peroxide (H_2O_2), nitrate (NO_3^-), and nitrite (NO_2^-) (Chu and Anastasio, 2005; Abbatt et al., 2010; Chu and Anastasio, 2007). Between 290–340 nm wavelengths, H_2O_2 has a wavelength-dependent molar absorptivity that is 2.5–7.1 times lower than that for NO_3^-. Nevertheless, H_2O_2 has a ≈ 160 times greater quantum yield for $^{\bullet}$OH production (Table 1) that is insensitive

to ionic strength, pH, and wavelength (Chu and Anastasio, 2005). Therefore, for a given concentration, H_2O_2 is a much more effective source of $^{\bullet}OH$ than nitrate. To our knowledge, the only H_2O_2 concentration value available at Dome C is 2 ng g^{-1}, derived from a sample collected at 3.5 m depth (Frey et al., 2006). This low value, compared to other locations, is consistent with semi-empirical models that predict a complete hydrogen peroxide loss when the accumulation rate is below ≈ 70 kg m^{-2} yr^{-1} and the annual mean temperature is $-50°$ (Frey et al., 2006). Considering that Dome C has an annual mean accumulation of $\approx$ 25–28 kg m^{-2} yr^{-1} (Genthon et al., 2016) and an annual mean temperature between -54 and $-50°$ (Genthon et al., 2021), we assume that the majority of the deposited or in situ-produced H_2O_2 is rapidly lost to the atmosphere.

Alternatively, NO_3 photolysis (Table 1), occurring at wavelengths of 290–340 nm, with a maximum at 320 nm (Winton et al., 2020), can act as a $^{\bullet}OH$ source, following the Reactions (R5)–(R8) (Chu and Anastasio, 2005; Abbatt et al., 2010; Boxe, 2005) as follows:

$$NO_3^- + h\nu \rightarrow NO_2^- + O^- \quad \text{(R5)}$$
$$O^- + H_2O \rightarrow {}^{\bullet}OH + OH^- \quad \text{(R6)}$$
$$H^+ + NO_2^- \rightarrow HONO \quad \text{(R7)}$$
$$HONO + h\nu \rightarrow {}^{\bullet}OH + NO. \quad \text{(R8)}$$

The $^{\bullet}OH$ radicals, formed by nitrate photolysis can produce $Br_{2(g)}$, following Reactions (R1)–(R4). The typical snowpack nitrate profile at Dome C ranges between 22 and 147 ng g^{-1} (Caiazzo et al., 2021; Spolaor et al., 2021) and shows an exponential decay in concentration with depth driven by nitrate UV photolysis and recycling (Winton et al., 2020; Röthlisberger et al., 2000; Savarino et al., 2007). Due to its higher concentration compared with hydrogen peroxide, nitrate may represent a relevant $^{\bullet}OH$ source at Dome C despite its lower quantum yield for $^{\bullet}OH$ production. The nitrate UV photolysis, followed by $^{\bullet}OH$ formation and $Br_{2(g)}$ emission, has been reported under laboratory conditions with a significant dependency on the ice pH, with the largest $Br_{2(g)}$ emissions observed at low pH (George and Anastasio, 2007).

Another source of OH radicals is nitrite (Minero et al., 2007), which can be produced by the dissociation of nitrous acid (HONO) in the condensed phase (Reaction R9),

$$HONO \leftrightarrow NO_2^- + H^+, \quad \text{(R9)}$$

or by the direct formation from the minor channel (quantum yield of approximately 0.0011) of nitrate photolysis (Reaction R5) (Dubowski et al., 2002).

Nitrite displays two major absorption bands peaking at 300 and 354 nm and, through its photolysis, it can produce $^{\bullet}OH$ (Reactions R10–R11) as follows:

$$NO_2^- + h\nu \rightarrow NO + {}^{\bullet}O^- \quad \text{(R10)}$$
$${}^{\bullet}O^- + H_2O \rightarrow {}^{\bullet}OH + OH^-. \quad \text{(R11)}$$

The $^{\bullet}OH$ quantum yield from nitrite photodissociation depends both on the wavelength (increases with decreasing wavelength) and on temperature (decreases with decreasing temperature). In addition, nitrite has a $\approx$ 2-fold higher molar absorptivity than nitrate between 280 and 300 nm (Chu and Anastasio, 2007) and its $^{\bullet}OH$ quantum yield in ice is equal to 0.020 (at 240 K, $\lambda = 300$), which is 6-fold higher than the one calculated for nitrate (Table 1). Unfortunately, there are no direct measurements of nitrite at Dome C, meaning that its concentration needs to be estimated. Following the approach used by Chu and Anastasio (2007), we assumed that at Dome C the nitrite concentration is similar to the one calculated at the South Pole, which is 0.092 ng g^{-1}. This assumption is based on: (a) similar superficial NO_3 concentrations recorded both at the South Pole (99 ng g^{-1}) and at Dome C (90–147 ng g^{-1}); (b) the use of NO_3^- photolysis as the main source for nitrite in the snow (Chu and Anastasio, 2007); and (c) the similar total UV radiation intensities and seasonality reaching both locations.

To evaluate the relevance of these processes on the OH radical production in the snow grains, and consequently their role in promoting $Br_{2(g)}$ emission from the snowpack, we modelled the hydrogen peroxide, nitrate, and nitrite photoactivation before (1950–1975) and after the ozone hole formation (post-1975) at Dome C, following the wavelength-dependent CAM-Chem model actinic flux output and the methodology described in Spolaor et al. (2021). Both H_2O_2 and NO_3^- exhibited a small, but significant, enhancement on their surface photolysis (J-value) after the onset of the ozone hole ($\approx$20 % increase) due to the higher actinic flux reaching the surface at λ<300 nm, where most of the H_2O_2 absorption occurs, and to a limited extent also NO_3^- (Figs. 3, 4). In contrast, NO_2^- does not show a significant trend on their J-values because both absorption bands maximise at longer wavelengths, within a spectral region that is not directly affected by the formation of the ozone hole (Figs. 3, 4). It is important to notice that the normalised photolysis ratio between the ozone hole period and the pre-ozone hole period strongly depends on the wavelength range considered to compute the J-value integration. For example, the ratio between the ozone hole and the pre-ozone hole periods for H_2O_2 ranges from a minimum value of 1.2 (280–390 nm) to a maximum value larger than 5 (280–300 nm) (Fig. S1). Equivalent results are obtained for the J-nitrate and J-nitrite enhancements (Fig. S1), although for these species, with the strongest absorption at longer wavelengths, the upper bandwidth limit used to perform the integration should not be located at values below 310–320 nm, which results in an up to 3-fold increase on the normalised ratio during the pre-ozone hole period. For these reasons, and based on the ob-

served molar absorptivities of each species shown in Fig. 3a, our best estimate of the normalised photolysis ratio shown in Fig. 4c was computed considering the following wavelengths ranges: 280–378 nm for H_2O_2, 295–357.5 nm for NO_3^-, and 280–390 nm for NO_2^-.

Taking into consideration the NO_3^-, H_2O_2, and NO_2^- concentrations at Dome C, and the $^\bullet$OH quantum yields from their photolysis (Table 1), we observed that the rates of $^\bullet$OH formation especially from the photolysis of H_2O_2 and NO_3^- slightly increased by a factor of 1.1 and 1.09 compared to the pre-ozone hole period, while for nitrite the enhancement was almost negligible (1.01). The average contribution of each of this species in producing OH radicals in the snow was the same both before and after the formation of the ozone hole; that is, 69 % from NO_3^-, 23 % from H_2O_2, and 8 % from NO_2^-. Specifically, the $^\bullet$OH formation rates during the ozone hole (pre-ozone hole) period from NO_3^-, H_2O_2, and NO_2^- photolysis are equal to 1.14×10^{-13} (1.05×10^{-13}) M s^{-1}, 3.80×10^{-13} (3.47×10^{-13}) M s^{-1}, and 1.2×10^{-14} (1.2×10^{-14}) M s^{-1}, respectively (Fig. 4b). Those values are calculated by multiplying the mean photolysis rate constant for $^\bullet$OH formation during the ozone hole (pre-ozone hole) period (i.e. 6.4×10^{-8} (5.9×10^{-8}) s^{-1} for NO_3^-, 5.9×10^{-6}, (5.36×10^{-7}) s^{-1} for H_2O_2, and 6.2×10^{-5} (6.2×10^{-6}) s^{-1} for NO_2^-) by the estimated or real snow grain concentration (110 ng g^{-1} or 1.77×10^{-6} M for NO_3^-, 2.2 ng g^{-1}, or 6.47×10^{-8} M for H_2O_2, and 0.092 ng g^{-1} or 2×10^{-9} M for NO_2^-). Our results are different from those computed at Neumayer station (Chu and Anastasio, 2007), where the dominant contributor to $^\bullet$OH production was H_2O_2 (2.3×10^{-11} M s^{-1}), followed by NO_3^- (3.9×10^{-13} M s^{-1}) and NO_2^- (1.8×10^{-13} M s^{-1}). Further, the $^\bullet$OH production rate at Dome C for H_2O_2 is 2 orders of magnitude lower than at Neumayer station, while it is similar for NO_3^-. The contribution of nitrite at Dome C is 1 order of magnitude lower than that computed at Neumayer station, where nitrite has been already considered as an insignificant source of $^\bullet$OH because of its very low estimated concentration (Chu and Anastasio, 2007). Overall, we can conclude that the contribution of H_2O_2, NO_3^-, and NO_2^- in forming OH radicals is low at Dome C both before and after the ozone hole period, and their change in photolysis is unlikely to have affected bromine preservation within the snowpack. This is in agreement with previous empirical observations (Legrand et al., 2016). We then propose that bromine release into the atmosphere can be favoured only in those locations where high snow acidity (e.g. in correspondence to a volcanic horizon or at coastal sites where biogenic marine emissions can enhance snow acidification) and high concentration of $^\bullet$OH precursors (e.g. H_2O_2) are found.

3.3 The role of volcanic eruptions in bromine preservation at Dome C

Volcanic eruptions are a significant halogen source with the emission of large amounts of HCl, HF, and HBr (Pyle and Mather, 2009). In particular, BrO formation through heterogeneous photochemical reactions was detected in a volcanic plume where local O_3 destruction occurred (Von Glasow et al., 2009). However, the role of volcanic eruptions in affecting bromine concentration in ice and snow has been poorly addressed. Studies performed in the European Alps (Legrand et al., 2021) and in the West Antarctic Ice Sheet Divide (Mcconnell et al., 2017), showed opposite results, with recorded bromine increase and depletion in coincidence with volcanic events, respectively. The Dome C shallow core presented in this work covers a period characterised by at least seven inter-hemispherical volcanic eruptions that were identified in other snow pits and deep cores, using both nssSO_4^{2-} and Fe(II) as volcanic proxies (Castellano et al., 2005; Burgay et al., 2021; Gautier et al., 2016): Pinatubo/Cerro Hudson (1991, VEI = 6), Agung (1963, VEI = 5), Krakatau (1886, VEI = 6), Cosiguina (1835, VEI = 5), Tambora (1815 = 7), and an unknown eruption (UE) 1809 (1809, VEI $\geq$ 5). VEI stands for Volcanic Explosivity Index, a commonly used quantity to define the magnitude of a volcanic eruption (Newhall and Self, 1982). Its values range from 0 (Hawaiian eruption) to 8 (ultra-Plinian eruption). In this record, we did not detect any clear fingerprint either as bromine increase or as depletion compared to the adjacent periods, suggesting a negligible role of volcanic eruptions in affecting the Br snow chemistry in the inland Antarctic plateau (Fig. S2). Nevertheless, we highlight that, due to low snow accumulation and to strong wind erosion, not all the volcanic eruptions listed above might be present in our record. Indeed, a previous investigation that compared the sulfate signal from five ice cores drilled 1 m apart from each other at Dome C showed a bulk probability of 30 % of missing volcanic events when a single core is used as the site reference (Gautier et al., 2016). Among the volcanic events embraced by our record, only Krakatau, Cosiguina, and UE 1809 were observed in all the previously mentioned five replicate cores, giving us confidence that for these eruptions the volcanic fingerprint is present also in our record. However, we acknowledge that a proxy-based volcanic reconstruction is missing for our core, and considering the strong spatial variability observed at Dome C, further and more specific studies are needed to investigate the impact of large inter-hemispherical volcanic eruptions on the preservation of bromine in the snowpack.

3.4 Can Br_{enr} at Dome C be used as proxy for past sea-ice extent?

Having presented evidence to demonstrate the preservation of bromine in the snowpack at Dome C and the absence of a link between our Br signal and the formation of the ozone

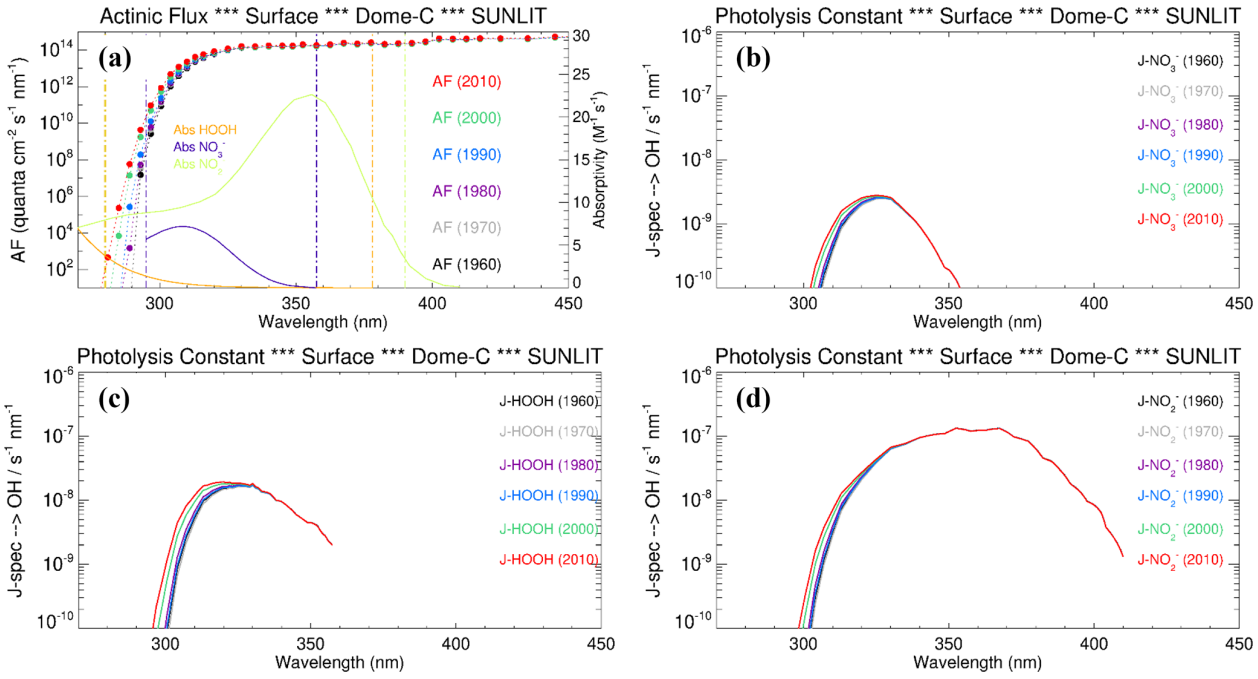

Figure 3. (a) The wavelength-dependent actinic flux (AF) at Dome C for different years (coloured dots), superimposed with the absorption spectrum of nitrate (violet line), hydrogen peroxide (orange line), and nitrite (green line). The photolysis rate for the main $^{\bullet}$OH precursors as a function of wavelength in different years (pre and post the modern ozone hole) is shown for **(b)** nitrate, **(c)** hydrogen peroxide, and **(d)** nitrite.

Table 2. Pearson correlations of 3 years moving average of Dome C Br, Na, and Br_{enr}, Law Dome MSA (MSA_{LD}) and seasonal sea-ice extents of the Indian Ocean (IO), western Pacific (WP), and Ross Sea (RS) sectors, and of the eastern Antarctic Ocean (EAO = IO + WP + RS), calculated as $FYSI = \overline{Extent}_{Sep-Dec} - Extent_{Feb}$. The moving average is calculated in order to account for a dating error of ~ 3 years. The correlations among the chemical species (Na, Br, Br_{enr}, and NO_3^-) were made over the entire record (1800–2012), the correlations with MSA_{LD} were done between 1843–1995, the correlations with SAM (Marshall index) were done between 1957–2012, and the correlations with sea-ice extents were done between 1979–2012.

	Na	Br	Br_{enr}	NO_3^-	MSA_{LD}	SAM	IO	WP	RS	EAO
Period	1800–2012				1843–1995	1957–2012	1979–2012			
Na	1.0***	0.06	−0.37***	0.53***	−0.04	0.61***	0.16	−0.2	0.74***	0.64***
Br	0.06	1.0***	0.76***	0.58***	−0.05	0.41***	0.36**	−0.24	0.44**	0.48***
Br_{enr}	−0.37***	0.76***	1.0***	0.45***	0.05	0.18	0.35*	−0.22	0.3*	0.35*
NO_3^-	0.53***	0.58***	0.45***	1.0***	0.04	0.24	0.3	−0.23	0.43**	0.44**
MSA_{LD}	−0.04	−0.05	0.05	0.04	1.0***	−0.08	−0.13	0.89***	0.32	0.58**
SAM	0.61***	0.41***	0.18	0.24	−0.08	1.0***	0.28	−0.14	0.58***	0.58***
IO	0.16	0.36**	0.35*	0.3	−0.13	0.28	1.0***	0.0	−0.06	0.42**
WP	−0.2	−0.24	−0.22	−0.23	0.89***	−0.14	0	1.0***	−0.03	0.31*
RS	0.74***	0.44**	0.3*	0.43**	0.32	0.58***	−0.06	−0.03	1.0***	0.82***
EAO	0.64***	0.48***	0.35*	0.44**	0.58**	0.58***	0.42**	0.31*	0.82***	1.0***

***: p-value ≤ 0.01; **: p-value ≤ 0.05; *: p-value ≤ 0.1.

hole, we now investigate the suitability of Dome C Br_{enr} as a proxy for past sea-ice variability. Previous studies supported the use of Br_{enr} in reconstructing past Antarctic sea-ice extent (Vallelonga et al., 2017; Spolaor et al., 2013b). However, these ice core records were retrieved at coastal sites close to local source areas, where Br_{enr} values where enriched with respect to sea water mass ratio. To the contrary, due to its position, Dome C receives atmospheric signals from a vast area of the East Antarctic sector (Fig. 1), which extends from the Indian Ocean to the Ross Sea, potentially giving a reconstruction of past-sea-ice extent over a broader region.

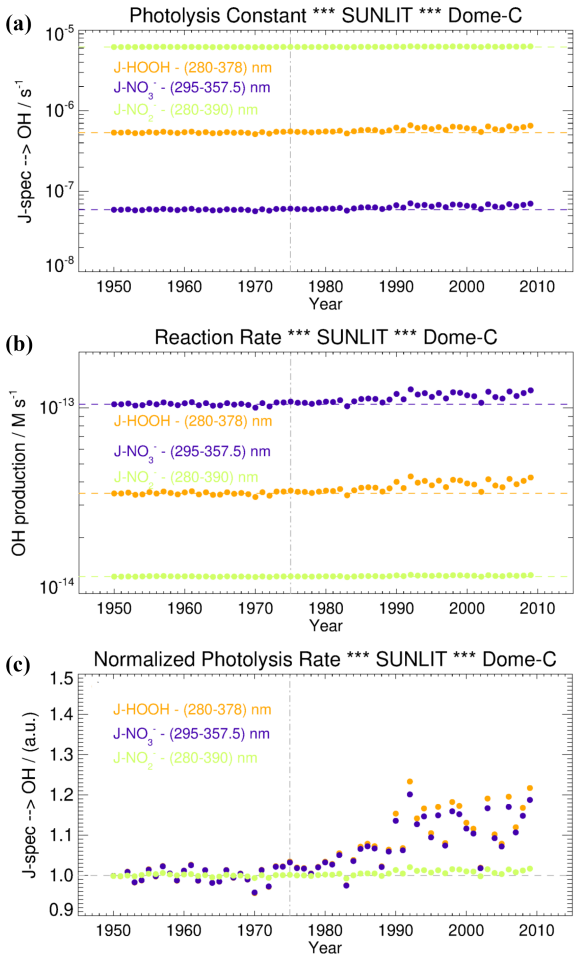

Figure 4. (a) The photolysis constant of hydrogen peroxide (orange line), nitrate (violet), and nitrite (green) over the period 1950–2009. **(b)** The $^{\bullet}$OH production rate after the hydrogen peroxide photolysis (orange), nitrate (violet), and nitrite (green) over the period 1950–2009. **(c)** Normalised photolysis rate for hydrogen peroxide photolysis (orange line), nitrate (violet line), and nitrite (green line) over the period 1950–2009. The dashed grey vertical line (1975) represents the beginning of the ozone hole period. The horizontal coloured lines represent the average magnitude during the pre-ozone hole period (1950–1975).

Our 200-year ice core record shows that Br_{enr} has an average value of 0.4 ± 0.3, meaning that it is typically depleted at Dome C. This reflects the differences in Na and Br depositions as a function of the distance from the coast, with resulting Br_{enr} values lower than 1 recorded at sites located more than 800 km far from the coast (Vallelonga et al., 2021). Further, due to the low snow accumulation at this location and to the low concentrations of bromine, Br_{enr} values can be influenced by surface snow removal by wind erosion, changes in meteorological patterns, and changes in wind field. For these reasons, and with the current state of knowledge, the presented bromine record should be interpreted with caution.

To understand the driving patterns of the Dome C record and its suitability to reconstruct past-sea-ice variability, we compare the Dome C Br_{enr} record with the annual averaged Southern Annular Mode (SAM) Marshall index (Marshall, 2003), satellite observations of FYSI extent from the source areas over the period 1979–2012, and with the Law Dome methanesulfonic acid (MSA_{LD}) profile (Curran et al., 2003) (Table 2). SAM describes the poleward/equatorward movement of the westerly winds that circle Antarctica. When these winds, known as southern westerly winds (SWWs), contract towards Antarctica, the SAM is in its positive phase, and vice versa in its negative phase. The strength of wind patterns likely influences the amount of sea salt aerosols deposited at Dome C (Crosta et al., 2021), as indicated by the positive correlation of Br and Na with SAM index (0.41 and 0.61, p-value <0.01, respectively). This is in agreement with recent findings that highlight a prominent northward flow during the SAM negative polarity at Dome C (Kino et al., 2021). We did not observe any correlation between the SAM index and Br_{enr} values.

We find that for the past decades, Br_{enr} at Dome C is mainly influenced by Br deposition, given the positive and significant correlation of Br_{enr} with total Br ($r = 0.76$, p-value ≤ 0.01) and the negative correlation with Na ($r = -0.37$, p-value ≤ 0.01) over the entire record (Table 2). Since gas-phase bromine is emitted in enhanced concentrations (with respect to sea water ratio) from sea salt aerosol derived from surface blowing snow deposited over FYSI, the Br_{enr} signal at Dome C is likely to be mainly controlled by emissions and recycling from seasonal sea ice at the Antarctic coast rather than long-range air mass transport of sea salt aerosols (Spolaor et al., 2013b).

To test this hypothesis, we compared our record with FYSI extent data (Parkinson and Cavalieri, 2012) during the satellite era (1979–2012) over the main source areas defined through back-trajectory analysis (Fig. 1). As previously stated, the large majority of the back trajectories that reaches Dome C over the period 1979–2018 originated from the WP sector (see Sect. 3.1, Fig. 1). However, we found significant but weak, correlations between Br_{enr} and FYSI only with the IO sector (11 % of the back-trajectory points satisfying bromine loading condition) and the RS (21 %) with $r = 0.35$ (p-value <0.1) and $r = 0.3$ (p-value <0.1), respectively. In contrast, the closer WP sector does not show any significant correlation with Br_{enr} (Table 2). Given the main source areas from back-trajectory analysis are located in the WP (45 %, Fig. 1), we further investigate this sector by considering the MSA record retrieved from the Law Dome ice core (hereafter MSA_{LD}), located at a coastal site facing the WP (Curran et al., 2003). MSA_{LD} shows a positive and significant correlation with the past-sea-ice extent in the WP sector ($r = 0.89$, p-value ≤ 0.01), but it does not correlate with Dome C Br_{enr}, strengthening the idea that Dome C is influenced by a broader source area than Law Dome. Based on these findings, a possible interpretation is that the IO and RS seasonal sea ice

might have a stronger influence on the Dome C Br_{enr} profile than WP, due to their 211 % and 157 % average larger FYSI extent than the one recorded in the WP (Fig. S3), leading to a larger emission of reactive bromine into the atmosphere. Overall, we found a weak, but significant, correlation between the Br_{enr} record and sea-ice extent in East Antarctica (WP + RS + IO) ($r = 0.35$, p-value ≤ 0.1). Nevertheless, we need to consider that overall sea-ice extent in East Antarctica has not undergone significant changes over the last 3 decades, with an interannual variability of ~ 20 %. Moreover, taking into account the observed Br_{enr} depletion at Dome C and the difficulties in capturing relatively small sea-ice variabilities due to snow remobilisation, and changes in meteorological patterns and in wind fields (Vallelonga et al., 2021), we hypothesise that sea-ice extent variability observed over the last decades has not been large enough to cause a significant variability in the Br_{enr} signal at Dome C. However, it cannot be ruled out that when longer periods which extend further back in the past are considered (e.g. glacial/interglacial transitions), Br_{enr} variations could be used as a qualitative tracer (i.e. to identify transitions between *large* and *small* FYSI extent) for FYSI variability in East Antarctica.

4 Conclusions

In this paper we presented the first long-term ice core record of bromine and bromine enrichment from Dome C (Antarctica). Based on observations and modelling results, we propose that bromine is effectively preserved within the Antarctic plateau snowpack regardless of the intensity of the incoming UV-radiation. Furthermore, we find that the change in surface UV-radiation due to ozone hole formation does not affect the contribution of H_2O_2, NO_3^- and NO_2^- to the production of OH radicals and consequently the dominant OH-driven bromide oxidation channel remains slow. We suggest that neither of these photochemical mechanisms are likely to take place at Dome C, mostly due to the low concentration of H_2O_2 and NO_2^- as well as the low $^\bullet$OH quantum yield from the NO_3^- photolysis. Due to the variety of chemical reactions that can influence bromine preservation within the snowpack, we suggest the inclusion of site-specific studies to assess to what extent bromine is preserved at different specific locations, i.e. through the analysis of $^\bullet$OH precursors (H_2O_2, NO_3^- and NO_2^-).

Finally, we provided preliminary insights on the effects of volcanic eruptions on the preservation of bromine in snow at Dome C, where we did not observe any influence on the Br record. However, due to the specific and peculiar environmental conditions at Dome C and to the lack of a proxy-based volcanic eruption reconstruction for this record, our findings are not conclusive and we encourage specific investigations on this topic. We also inquired whether Br_{enr} at Dome C can be used as a sea-ice proxy for the East Antarctic sector. Despite finding weak – but significant – correlations with the Indian Ocean and Ross Sea sectors (which are the ones presenting the largest FYSI extents) it is difficult to validate Br_{enr} as an effective proxy for past sea-ice reconstructions in East Antarctica; this is primarily due to low sea-ice variability observed during the last 30 years. Future investigations at Dome C need to focus on glacial/interglacial transitions to assess whether Br_{enr} at Dome C is somehow related to large-scale variations of sea-ice extensions.

Code availability. The software code for the Community Earth System Model (CESM) is available from https://www.cesm.ucar.edu/models/cesm2 (NCAR, 2022.).

Data availability. Na, Br, and Brenr data are available at https://doi.org/10.5281/zenodo.7565059 (Burgay et al., 2023).

Supplement. The supplement related to this article is available online at: https://doi.org/10.5194/tc-17-391-2023-supplement.

Author contributions. FB: conceptualisation, data curation, formal analysis, investigation, methodology, visualisation, and writing (original draft preparation). RPF: data curation, formal analysis, investigation, methodology, software, visualisation, and writing (original draft preparation and review and editing). DS: data curation, formal analysis, methodology, software, visualisation, and writing (original draft preparation and review and editing). CT: data curation, methodology, and writing (review and editing). CSBB: writing (review and editing). RHR: writing (review and editing). CS: software and writing (review and editing). VC: software and writing (review and editing). CB: funding acquisition, supervision, and writing (review and editing). ASL: investigation and writing (review and editing). AS: conceptualisation, investigation, resources, supervision, and writing (review and editing).

Competing interests. The contact author has declared that none of the authors has any competing interests.

Disclaimer. Publisher's note: Copernicus Publications remains neutral with regard to jurisdictional claims in published maps and institutional affiliations.

Acknowledgements. This publication has been generated in the frame of Beyond EPICA. Logistic support has mainly been provided by PNRA and IPEV through the Concordia Station system. We acknowledge Massimo Frezzotti, for providing us physical snow data from Dome C. This is Beyond EPICA publication number 29.

Financial support. This research has been supported by the Horizon 2020 (Beyond EPICA; grant no. 815384), by the Programma Nazionale per la Ricerca in Antartide (PNRA; project no. PNRA16_00295), and by the bilateral international exchange award Royal Society (UK)-CNR, titled "Antarctic sea-ice history: developing robust ice core proxies" (grant no. IEC/R2/202110), awarded to Rachael H. Rhodes and Andrea Spolaor.

Review statement. This paper was edited by Florence Colleoni and reviewed by two anonymous referees.

References

Abbatt, J., Oldridge, N., Symington, A., Chukalovskiy, V., McWhinney, R., Sjostedt, S., and Cox, R.: Release of gas-phase halogens by photolytic generation of OH in frozen halide- nitrate solutions: an active halogen formation mechanism?, J. Phys. Chem. A, 114, 6527–6533, 2010.

Artiglia, L., Edebeli, J., Orlando, F., Chen, S., Lee, M.-T., Arroyo, P. C., Gilgen, A., Bartels-Rausch, T., Kleibert, A., and Vazdar, M.: A surface-stabilized ozonide triggers bromide oxidation at the aqueous solution-vapour interface, Nat. Commun., 8, 1–8, 2017.

Barrie, L., Bottenheim, J., Schnell, R., Crutzen, P., and Rasmussen, R.: Ozone destruction and photochemical reactions at polar sunrise in the lower Arctic atmosphere, Nature, 334, 138–141, 1988.

Becagli, S., Marchese, C., Caiazzo, L., Ciardini, V., Lazzara, L., Mori, G., Nuccio, C., Scarchilli, C., Severi, M., and Traversi, R.: Biogenic aerosol in central East Antarctic Plateau as a proxy for the ocean-atmosphere interaction in the Southern Ocean, Sci. Total Environ., 810, 151285, https://doi.org/10.1016/j.scitotenv.2021.151285, 2022.

Boxe, C.: Nitrate photochemistry and interrelated chemical phenomena in ice, California Institute of Technology, https://doi.org/10.7907/NC6C-NA28, 2005.

Burgay, F., Barbaro, E., Cappelletti, D., Turetta, C., Gallet, J.-C., Isaksson, E., Stenni, B., Dreossi, G., Scoto, F., and Barbante, C.: First discrete iron (II) records from Dome C (Antarctica) and the Holtedahlfonna glacier (Svalbard), Chemosphere, 267, 129335, https://doi.org/10.1016/j.chemosphere.2020.129335, 2021.

Burgay, F., Fernandez, R. P., Segato, D., Turetta, C., Blaszczak-Boxe, C., Rhodes, R., Scarchilli, C., Ciardini, V., Barbante, C., Saiz-Lopez, A., and Spolaor, A.: 200-years ice core bromine reconstruction at Dome C (Antarctica): observational and modelling results, in: The Cryosphere, Zenodo [data set], https://doi.org/10.5281/zenodo.7565059, 2023.

Caiazzo, L., Becagli, S., Bertinetti, S., Grotti, M., Nava, S., Severi, M., and Traversi, R.: High Resolution Chemical Stratigraphies of Atmospheric Depositions from a 4 m Depth Snow Pit at Dome C (East Antarctica), Atmosphere, 12, 909, https://doi.org/10.3390/atmos12070909, 2021.

Cairns, W. R., Turetta, C., Maffezzoli, N., Magand, O., Araujo, B. F., Angot, H., Segato, D., Cristofanelli, P., Sprovieri, F., and Scarchilli, C.: Mercury in precipitated and surface snow at Dome C and a first estimate of mercury depositional fluxes during the Austral summer on the high Antarctic plateau, Atmos. Environ., 262, 118634, https://doi.org/10.1016/J.Atmosenv.2021.118634, 2021.

Carpenter, L. J., MacDonald, S. M., Shaw, M. D., Kumar, R., Saunders, R. W., Parthipan, R., Wilson, J., and Plane, J. M.: Atmospheric iodine levels influenced by sea surface emissions of inorganic iodine, Nat. Geosci., 6, 108–111, 2013.

Castellano, E., Becagli, S., Hansson, M., Hutterli, M., Petit, J., Rampino, M., Severi, M., Steffensen, J. P., Traversi, R., and Udisti, R.: Holocene volcanic history as recorded in the sulfate stratigraphy of the European Project for Ice Coring in Antarctica Dome C (EDC96) ice core, J. Geophys. Res.-Atmos., 110, D06114, https://doi.org/10.1029/2004JD005259, 2005.

Chu, L. and Anastasio, C.: Quantum yields of hydroxyl radical and nitrogen dioxide from the photolysis of nitrate on ice, J. Phys. Chem. A, 107, 9594–9602, 2003.

Chu, L. and Anastasio, C.: Formation of hydroxyl radical from the photolysis of frozen hydrogen peroxide, J. Phys. Chem. A, 109, 6264–6271, 2005.

Chu, L. and Anastasio, C.: Temperature and wavelength dependence of nitrite photolysis in frozen and aqueous solutions, Environ. Sci. Technol., 41, 3626–3632, 2007.

Crosta, X., Etourneau, J., Orme, L. C., Dalaiden, Q., Campagne, P., Swingedouw, D., Goosse, H., Massé, G., Miettinen, A., and McKay, R. M.: Multi-decadal trends in Antarctic sea-ice extent driven by ENSO–SAM over the last 2,000 years, Nat. Geosci., 14, 156–160, 2021.

Cuevas, C. A., Maffezzoli, N., Corella, J. P., Spolaor, A., Vallelonga, P., Kjær, H. A., Simonsen, M., Winstrup, M., Vinther, B., and Horvat, C.: Rapid increase in atmospheric iodine levels in the North Atlantic since the mid-20th century, Nat. Commun., 9, 1–6, 2018.

Curran, M. A., van Ommen, T. D., Morgan, V. I., Phillips, K. L., and Palmer, A. S.: Ice core evidence for Antarctic sea ice decline since the 1950s, Science, 302, 1203–1206, 2003.

Dibb, J. E., Ziemba, L. D., Luxford, J., and Beckman, P.: Bromide and other ions in the snow, firn air, and atmospheric boundary layer at Summit during GSHOX, Atmos. Chem. Phys., 10, 9931–9942, https://doi.org/10.5194/acp-10-9931-2010, 2010.

Dubowski, Y., Colussi, A., Boxe, C., and Hoffmann, M.: Monotonic increase of nitrite yields in the photolysis of nitrate in ice and water between 238 and 294 K, J. Phys. Chem. A, 106, 6967–6971, 2002.

Eyring, V., Lamarque, J.-F., Hess, P., Arfeuille, F., Bowman, K., Chipperfiel, M. P., Duncan, B., Fiore, A., Gettelman, A., and Giorgetta, M. A.: Overview of IGAC/SPARC Chemistry-Climate Model Initiative (CCMI) community simulations in support of upcoming ozone and climate assessments, SPARC newsletter, 40, 48–66, 2013.

Fan, S.-M. and Jacob, D. J.: Surface ozone depletion in Arctic spring sustained by bromine reactions on aerosols, Nature, 359, 522–524, 1992.

Fernandez, R. P., Salawitch, R. J., Kinnison, D. E., Lamarque, J.-F., and Saiz-Lopez, A.: Bromine partitioning in the tropical tropopause layer: implications for stratospheric injection, Atmos. Chem. Phys., 14, 13391–13410, https://doi.org/10.5194/acp-14-13391-2014, 2014.

Fernandez, R. P., Kinnison, D. E., Lamarque, J.-F., Tilmes, S., and Saiz-Lopez, A.: Impact of biogenic very short-lived bromine on the Antarctic ozone hole during the 21st century, Atmos. Chem. Phys., 17, 1673–1688, https://doi.org/10.5194/acp-17-1673-2017, 2017.

Fernandez, R. P., Barrera, J. A., López-Noreña, A. I., Kinnison, D. E., Nicely, J., Salawitch, R. J., Wales, P. A., Toselli, B. M., Tilmes, S., and Lamarque, J. F.: Intercomparison Between Surrogate, Explicit, and Full Treatments of VSL Bromine Chemistry Within the CAM-Chem Chemistry-Climate Model, Geophys. Res. Lett., 48, e2020GL091125, https://doi.org/10.1029/2020GL091125, 2021.

Fernandez, R. P., Carmona-Balea, A., Cuevas, C. A., Barrera, J. A., Kinnison, D. E., Lamarque, J. F., Blaszczak-Boxe, C., Kim, K., Choi, W., and Hay, T.: Modeling the sources and chemistry of polar tropospheric halogens (Cl, Br, and I) using the CAM-Chem Global Chemistry-Climate Model, J. Adv. Model. Earth Sy., 11, 2259–2289, 2019.

Flores, E. M., Mello, P. A., Krzyzaniak, S. R., Cauduro, V. H., and Picoloto, R. S.: Challenges and trends for halogen determination by inductively coupled plasma mass spectrometry: a review, Rapid Commun. Mass. Sp., 34, e8727, https://doi.org/10.1002/rcm.8727, 2020.

Foster, K. L., Plastridge, R. A., Bottenheim, J. W., Shepson, P. B., Finlayson-Pitts, B. J., and Spicer, C. W.: The role of Br_2 and BrCl in surface ozone destruction at polar sunrise, Science, 291, 471–474, 2001.

Frey, M. M., Bales, R. C., and McConnell, J. R.: Climate sensitivity of the century-scale hydrogen peroxide (H_2O_2) record preserved in 23 ice cores from West Antarctica, J. Geophys. Res.-Atmos., 111, D21301, https://doi.org/10.1029/2005JD006816, 2006.

Frey, M. M., Savarino, J., Morin, S., Erbland, J., and Martins, J. M. F.: Photolysis imprint in the nitrate stable isotope signal in snow and atmosphere of East Antarctica and implications for reactive nitrogen cycling, Atmos. Chem. Phys., 9, 8681–8696, https://doi.org/10.5194/acp-9-8681-2009, 2009.

Frey, M. M., Norris, S. J., Brooks, I. M., Anderson, P. S., Nishimura, K., Yang, X., Jones, A. E., Nerentorp Mastromonaco, M. G., Jones, D. H., and Wolff, E. W.: First direct observation of sea salt aerosol production from blowing snow above sea ice, Atmos. Chem. Phys., 20, 2549–2578, https://doi.org/10.5194/acp-20-2549-2020, 2020.

Frezzotti, M., Scarchilli, C., Becagli, S., Proposito, M., and Urbini, S.: A synthesis of the Antarctic surface mass balance during the last 800 yr, The Cryosphere, 7, 303–319, https://doi.org/10.5194/tc-7-303-2013, 2013.

Frezzotti, M., Pourchet, M., Flora, O., Gandolfi, S., Gay, M., Urbini, S., Vincent, C., Becagli, S., Gragnani, R., Proposito, M., Severi, M., Traversi, R., Udisti, R., and Fily, M.: Spatial and temporal variability of snow accumulation in East Antarctica from traverse data, J. Glaciol., 51, 113–124, https://doi.org/10.3189/172756505781829502, 2005.

Gautier, E., Savarino, J., Erbland, J., Lanciki, A., and Possenti, P.: Variability of sulfate signal in ice core records based on five replicate cores, Clim. Past, 12, 103–113, https://doi.org/10.5194/cp-12-103-2016, 2016.

Genthon, C., Six, D., Scarchilli, C., Ciardini, V., and Frezzotti, M.: Meteorological and snow accumulation gradients across Dome C, East Antarctic plateau, Int. J. Climatol., 36, 455–466, 2016.

Genthon, C., Veron, D., Vignon, E., Six, D., Dufresne, J.-L., Madeleine, J.-B., Sultan, E., and Forget, F.: 10 years of temperature and wind observation on a 45 m tower at Dome C, East Antarctic plateau, Earth Syst. Sci. Data, 13, 5731–5746, https://doi.org/10.5194/essd-13-5731-2021, 2021.

George, I. J. and Anastasio, C.: Release of gaseous bromine from the photolysis of nitrate and hydrogen peroxide in simulated sea-salt solutions, Atmos. Enviro., 41, 543–553, 2007.

Grannas, A. M., Jones, A. E., Dibb, J., Ammann, M., Anastasio, C., Beine, H. J., Bergin, M., Bottenheim, J., Boxe, C. S., Carver, G., Chen, G., Crawford, J. H., Dominé, F., Frey, M. M., Guzmán, M. I., Heard, D. E., Helmig, D., Hoffmann, M. R., Honrath, R. E., Huey, L. G., Hutterli, M., Jacobi, H. W., Klán, P., Lefer, B., McConnell, J., Plane, J., Sander, R., Savarino, J., Shepson, P. B., Simpson, W. R., Sodeau, J. R., von Glasow, R., Weller, R., Wolff, E. W., and Zhu, T.: An overview of snow photochemistry: evidence, mechanisms and impacts, Atmos. Chem. Phys., 7, 4329–4373, https://doi.org/10.5194/acp-7-4329-2007, 2007.

Gutmann, A., Bobrowski, N., Roberts, T. J., Rüdiger, J., and Hoffmann, T.: Advances in bromine speciation in volcanic plumes, Front. Earth Sci., 6, 213, https://doi.org/10.3389/feart.2018.00213, 2018.

Hersbach, H., Bell, B., Berrisford, P., Hirahara, S., Horányi, A., Muñoz-Sabater, J., Nicolas, J., Peubey, C., Radu, R., and Schepers, D.: The ERA5 global reanalysis, Q. J. Roy. Meteor. Soc., 146, 1999–2049, 2020.

Kim, K., Yabushita, A., Okumura, M., Saiz-Lopez, A., Cuevas, C. A., Blaszczak-Boxe, C. S., Min, D. W., Yoon, H.-I., and Choi, W.: Production of molecular iodine and tri-iodide in the frozen solution of iodide: implication for polar atmosphere, Environ. Sci. Technol., 50, 1280–1287, 2016.

Kino, K., Okazaki, A., Cauquoin, A., and Yoshimura, K.: Contribution of the Southern Annular Mode to variations in water isotopes of daily precipitation at Dome Fuji, East Antarctica, J. Geophys. Res.-Atmos., 126, e2021JD035397, https://doi.org/10.1029/2021JD035397, 2021.

Kreher, K., Johnston, P., Wood, S., Nardi, B., and Platt, U.: Ground-based measurements of tropospheric and stratospheric BrO at Arrival Heights, Antarctica, Geophys. Res. Lett., 24, 3021–3024, 1997.

Legrand, M., Yang, X., Preunkert, S., and Theys, N.: Year-round records of sea salt, gaseous, and particulate inorganic bromine in the atmospheric boundary layer at coastal (Dumont d'Urville) and central (Concordia) East Antarctic sites, J. Geophy. Res.-Atmos., 121, 997–1023, 2016.

Legrand, M., McConnell, J., Preunkert, S., Chellman, N., and Arienzo, M.: Causes of enhanced bromine levels in Alpine ice cores during the 20th century: Implications for bromine in the free European troposphere, J. Geophys. Res.-Atmos., 126, e2020JD034246, https://doi.org/10.1029/2020JD034246, 2021.

Lewis, E. R., Lewis, R., Lewis, E. R., and Schwartz, S. E.: Sea salt aerosol production: mechanisms, methods, measurements, and models, American Geophysical Union, 426 pp., ISBN 9780875904177, 2004.

Maffezzoli, N., Vallelonga, P., Edwards, R., Saiz-Lopez, A., Turetta, C., Kjær, H. A., Barbante, C., Vinther, B., and Spolaor, A.: A 120 000-year record of sea ice in the North Atlantic?, Clim. Past, 15, 2031–2051, https://doi.org/10.5194/cp-15-2031-2019, 2019.

Marshall, G. J.: Trends in the Southern Annular Mode from observations and reanalyses, J. Climate, 16, 4134–4143, 2003.

Maselli, O. J., Chellman, N. J., Grieman, M., Layman, L., McConnell, J. R., Pasteris, D., Rhodes, R. H., Saltzman, E., and Sigl, M.: Sea ice and pollution-modulated changes in Greenland

ice core methanesulfonate and bromine, Clim. Past, 13, 39–59, https://doi.org/10.5194/cp-13-39-2017, 2017.

McConnell, J. R., Burke, A., Dunbar, N. W., Köhler, P., Thomas, J. L., Arienzo, M. M., Chellman, N. J., Maselli, O. J., Sigl, M., and Adkins, J. F.: Synchronous volcanic eruptions and abrupt climate change ∼ 17.7 ka plausibly linked by stratospheric ozone depletion, P. Natl. Acad Sci. USA, 114, 10035–10040, 2017.

Millero, F. J., Feistel, R., Wright, D. G., and McDougall, T. J.: The composition of Standard Seawater and the definition of the Reference-Composition Salinity Scale, Deep Sea Research Part I: Oceanographic Research Papers, 55, 50–72, 2008.

Minero, C., Chiron, S., Falletti, G., Maurino, V., Pelizzetti, E., Ajassa, R., Carlotti, M. E., and Vione, D.: Photochemincal processes involving nitrite in surface water samples, Aquat. Sci., 69, 71–85, 2007.

NCAR: The software code for the Community Earth System Model (CESM), https://www.cesm.ucar.edu/models/cesm2, last access: 25 January 2022.

Newhall, C. G. and Self, S.: The volcanic explosivity index (VEI) an estimate of explosive magnitude for historical volcanism, J. Geophys. Res.-Oceans, 87, 1231–1238, 1982.

Nghiem, S. V., Rigor, I. G., Richter, A., Burrows, J. P., Shepson, P. B., Bottenheim, J., Barber, D. G., Steffen, A., Latonas, J., and Wang, F.: Field and satellite observations of the formation and distribution of Arctic atmospheric bromine above a rejuvenated sea ice cover, J. Geophys. Res.-Atmos., 117, D00S05, https://doi.org/10.1029/2011JD016268, 2012.

Ordóñez, C., Lamarque, J.-F., Tilmes, S., Kinnison, D. E., Atlas, E. L., Blake, D. R., Sousa Santos, G., Brasseur, G., and Saiz-Lopez, A.: Bromine and iodine chemistry in a global chemistry-climate model: description and evaluation of very short-lived oceanic sources, Atmos. Chem. Phys., 12, 1423–1447, https://doi.org/10.5194/acp-12-1423-2012, 2012.

Parkinson, C. L. and Cavalieri, D. J.: Antarctic sea ice variability and trends, 1979–2010, The Cryosphere, 6, 871–880, https://doi.org/10.5194/tc-6-871-2012, 2012.

Parrella, J. P., Jacob, D. J., Liang, Q., Zhang, Y., Mickley, L. J., Miller, B., Evans, M. J., Yang, X., Pyle, J. A., Theys, N., and Van Roozendael, M.: Tropospheric bromine chemistry: implications for present and pre-industrial ozone and mercury, Atmos. Chem. Phys., 12, 6723–6740, https://doi.org/10.5194/acp-12-6723-2012, 2012.

Picard, G., Arnaud, L., Caneill, R., Lefebvre, E., and Lamare, M.: Observation of the process of snow accumulation on the Antarctic Plateau by time lapse laser scanning, The Cryosphere, 13, 1983–1999, https://doi.org/10.5194/tc-13-1983-2019, 2019.

Platt, U. and Lehrer, E.: ARCTOC Final Report to the European Union, 1997.

Prados-Roman, C., Cuevas, C. A., Fernandez, R. P., Kinnison, D. E., Lamarque, J.-F., and Saiz-Lopez, A.: A negative feedback between anthropogenic ozone pollution and enhanced ocean emissions of iodine, Atmos. Chem. Phys., 15, 2215–2224, https://doi.org/10.5194/acp-15-2215-2015, 2015.

Pratt, K. A., Custard, K. D., Shepson, P. B., Douglas, T. A., Pöhler, D., General, S., Zielcke, J., Simpson, W. R., Platt, U., and Tanner, D. J.: Photochemical production of molecular bromine in Arctic surface snowpacks, Nat. Geosci., 6, 351–356, 2013.

Pyle, D. and Mather, T.: Halogens in igneous processes and their fluxes to the atmosphere and oceans from volcanic activity: A review, Chem. Geol., 263, 110–121, 2009.

Röthlisberger, R., Hutterli, M. A., Sommer, S., Wolff, E. W., and Mulvaney, R.: Factors controlling nitrate in ice cores: Evidence from the Dome C deep ice core, J. Geophys. Res.-Atmos., 105, 20565–20572, 2000.

Saiz-Lopez, A. and von Glasow, R.: Reactive halogen chemistry in the troposphere, Chem. Soc. Rev., 41, 6448–6472, 2012.

Saiz-Lopez, A. and Fernandez, R. P.: On the formation of tropical rings of atomic halogens: Causes and implications, Geophys. Res. Lett., 43, 2928–2935, 2016.

Sander, R., Keene, W. C., Pszenny, A. A. P., Arimoto, R., Ayers, G. P., Baboukas, E., Cainey, J. M., Crutzen, P. J., Duce, R. A., Hönninger, G., Huebert, B. J., Maenhaut, W., Mihalopoulos, N., Turekian, V. C., and Van Dingenen, R.: Inorganic bromine in the marine boundary layer: a critical review, Atmos. Chem. Phys., 3, 1301–1336, https://doi.org/10.5194/acp-3-1301-2003, 2003.

Savarino, J., Kaiser, J., Morin, S., Sigman, D. M., and Thiemens, M. H.: Nitrogen and oxygen isotopic constraints on the origin of atmospheric nitrate in coastal Antarctica, Atmos. Chem. Phys., 7, 1925–1945, https://doi.org/10.5194/acp-7-1925-2007, 2007.

Schönhardt, A., Begoin, M., Richter, A., Wittrock, F., Kaleschke, L., Gómez Martín, J. C., and Burrows, J. P.: Simultaneous satellite observations of IO and BrO over Antarctica, Atmos. Chem. Phys., 12, 6565–6580, https://doi.org/10.5194/acp-12-6565-2012, 2012.

Simpson, W. R., Alvarez-Aviles, L., Douglas, T. A., Sturm, M., and Domine, F.: Halogens in the coastal snow pack near Barrow, Alaska: Evidence for active bromine air-snow chemistry during springtime, Geophys. Res. Lett., 32, L04811, https://doi.org/10.1029/2004GL021748, 2005.

Simpson, W. R., von Glasow, R., Riedel, K., Anderson, P., Ariya, P., Bottenheim, J., Burrows, J., Carpenter, L. J., Frieß, U., Goodsite, M. E., Heard, D., Hutterli, M., Jacobi, H.-W., Kaleschke, L., Neff, B., Plane, J., Platt, U., Richter, A., Roscoe, H., Sander, R., Shepson, P., Sodeau, J., Steffen, A., Wagner, T., and Wolff, E.: Halogens and their role in polar boundary-layer ozone depletion, Atmos. Chem. Phys., 7, 4375–4418, https://doi.org/10.5194/acp-7-4375-2007, 2007.

Song, S., Angot, H., Selin, N. E., Gallée, H., Sprovieri, F., Pirrone, N., Helmig, D., Savarino, J., Magand, O., and Dommergue, A.: Understanding mercury oxidation and air–snow exchange on the East Antarctic Plateau: a modeling study, Atmos. Chem. Phys., 18, 15825–15840, https://doi.org/10.5194/acp-18-15825-2018, 2018.

Spolaor, A., Vallelonga, P., Gabrieli, J., Kehrwald, N., Turetta, C., Cozzi, G., Poto, L., Plane, J., Boutron, C., and Barbante, C.: Speciation analysis of iodine and bromine at picogram-per-gram levels in polar ice, Anal. Bioanal. Chem., 405, 647–654, 2013a.

Spolaor, A., Vallelonga, P., Plane, J. M. C., Kehrwald, N., Gabrieli, J., Varin, C., Turetta, C., Cozzi, G., Kumar, R., Boutron, C., and Barbante, C.: Halogen species record Antarctic sea ice extent over glacial–interglacial periods, Atmos. Chem. Phys., 13, 6623–6635, https://doi.org/10.5194/acp-13-6623-2013, 2013b.

Spolaor, A., Vallelonga, P., Turetta, C., Maffezzoli, N., Cozzi, G., Gabrieli, J., Barbante, C., Goto-Azuma, K., Saiz-Lopez, A., Cuevas, C. A., and Dahl-Jensen, D.: Canadian Arctic sea ice re-

constructed from bromine in the Greenland NEEM ice core, Sci. Rep., 6, 33925, https://doi.org/10.1038/srep33925, 2016.

Spolaor, A., Angot, H., Roman, M., Dommergue, A., Scarchilli, C., Vardè, M., Del Guasta, M., Pedeli, X., Varin, C., and Sprovieri, F.: Feedback mechanisms between snow and atmospheric mercury: Results and observations from field campaigns on the Antarctic plateau, Chemosphere, 197, 306–317, 2018.

Spolaor, A., Barbaro, E., Cappelletti, D., Turetta, C., Mazzola, M., Giardi, F., Björkman, M. P., Lucchetta, F., Dallo, F., Pfaffhuber, K. A., Angot, H., Dommergue, A., Maturilli, M., Saiz-Lopez, A., Barbante, C., and Cairns, W. R. L.: Diurnal cycle of iodine, bromine, and mercury concentrations in Svalbard surface snow, Atmos. Chem. Phys., 19, 13325–13339, https://doi.org/10.5194/acp-19-13325-2019, 2019.

Spolaor, A., Burgay, F., Fernandez, R. P., Turetta, C., Cuevas, C. A., Kim, K., Kinnison, D. E., Lamarque, J.-F., de Blasi, F., Barbaro, E., Corella, J. P., Vallelonga, P., Frezzotti, M., Barbante, C., and Saiz-Lopez, A.: Antarctic ozone hole modifies iodine geochemistry on the Antarctic Plateau, Nat. Commun., 12, 5836, https://doi.org/10.1038/s41467-021-26109-x, 2021.

Stein, A., Draxler, R. R., Rolph, G. D., Stunder, B. J., Cohen, M., and Ngan, F.: NOAA's HYSPLIT atmospheric transport and dispersion modeling system, B. Am. Meteorol. Soc., 96, 2059–2077, 2015.

Tilmes, S., Lamarque, J.-F., Emmons, L. K., Kinnison, D. E., Marsh, D., Garcia, R. R., Smith, A. K., Neely, R. R., Conley, A., Vitt, F., Val Martin, M., Tanimoto, H., Simpson, I., Blake, D. R., and Blake, N.: Representation of the Community Earth System Model (CESM1) CAM4-chem within the Chemistry-Climate Model Initiative (CCMI), Geosci. Model Dev., 9, 1853–1890, https://doi.org/10.5194/gmd-9-1853-2016, 2016.

Vallelonga, P., Maffezzoli, N., Moy, A. D., Curran, M. A. J., Vance, T. R., Edwards, R., Hughes, G., Barker, E., Spreen, G., Saiz-Lopez, A., Corella, J. P., Cuevas, C. A., and Spolaor, A.: Sea-ice-related halogen enrichment at Law Dome, coastal East Antarctica, Clim. Past, 13, 171–184, https://doi.org/10.5194/cp-13-171-2017, 2017.

Vallelonga, P., Maffezzoli, N., Saiz-Lopez, A., Scoto, F., Kjær, H. A., and Spolaor, A.: Sea-ice reconstructions from bromine and iodine in ice cores, Quaternary Sci. Rev., 269, 107133, https://doi.org/10.1016/j.quascirev.2021.107133, 2021.

Vogt, R., Crutzen, P. J., and Sander, R.: A mechanism for halogen release from sea-salt aerosol in the remote marine boundary layer, Nature, 383, 327–330, 1996.

von Glasow, R., Bobrowski, N., and Kern, C.: The effects of volcanic eruptions on atmospheric chemistry, Chem. Geol., 263, 131–142, 2009.

Wennberg, P.: Bromine explosion, Nature, 397, 299–301, 1999.

Winton, V. H. L., Ming, A., Caillon, N., Hauge, L., Jones, A. E., Savarino, J., Yang, X., and Frey, M. M.: Deposition, recycling, and archival of nitrate stable isotopes between the air–snow interface: comparison between Dronning Maud Land and Dome C, Antarctica, Atmos. Chem. Phys., 20, 5861–5885, https://doi.org/10.5194/acp-20-5861-2020, 2020.

Yang, X., Cox, R. A., Warwick, N. J., Pyle, J. A., Carver, G. D., O'Connor, F. M., and Savage, N. H.: Tropospheric bromine chemistry and its impacts on ozone: A model study, J. Geophys. Res.-Atmos., 110, D23311, https://doi.org/10.1029/2005JD006244, 2005.

Zhao, X., Strong, K., Adams, C., Schofield, R., Yang, X., Richter, A., Friess, U., Blechschmidt, A. M., and Koo, J. H.: A case study of a transported bromine explosion event in the Canadian high arctic, J. Geophys. Res.-Atmos., 121, 457–477, 2016.